JOURNAL OF THE ROYAL SOCIETY Interface

J. R. Soc. Interface (2011) **8**, 926–933
doi:10.1098/rsif.2010.0720
Published online 2 February 2011

Orientation angle and the adhesion of single gecko setae

Ginel C. Hill[1,*,†], Daniel R. Soto[1], Anne M. Peattie[3], Robert J. Full[3] and T. W. Kenny[2]

[1]*Department of Applied Physics, and* [2]*Department of Mechanical Engineering, Stanford University, Stanford, CA 94305, USA*
[3]*Department of Integrative Biology, University of California, Berkeley, Berkeley, CA 94720, USA*

We investigated the effects of orientation angle on the adhesion of single gecko setae using dual-axis microelectromechanical systems force sensors to simultaneously detect normal and shear force components. Adhesion was highly sensitive to the pitch angle between the substrate and the seta's stalk. Maximum lateral adhesive force was observed with the stalk parallel to the substrate, and adhesion decreased smoothly with increasing pitch. The roll orientation angle only needed to be roughly correct with the spatular tuft of the seta oriented grossly towards the substrate for high adhesion. Also, detailed measurements were made to control for the effect of normal preload forces. Higher normal preload forces caused modest enhancement of the observed lateral adhesive force, provided that adequate contact was made between the seta and the substrate. These results should be useful in the design and manufacture of gecko-inspired synthetic adhesives with anisotropic properties, an area of substantial recent research efforts.

Keywords: gecko; adhesion; single seta; force sensing; dual axis

1. INTRODUCTION

Geckos possess marvellous abilities of adhesion that enable them to run upside down, to manoeuvre on a wide variety of substrates and to arrest their falls. These skills are made possible by a complex and hierarchical adhesion system featuring fine keratin hairs, called setae, that densely cover the gecko's foot pads. Setae branch at their distal end into hundreds of even finer fibres that each terminate in a flattened structure called a 'spatula'. These spatulae make intimate contact with the substrate [1,2]. By the shear number of contact points achieved through this hierarchical structure, attractive intermolecular forces at each contact point contribute to macroscopic adhesion forces between setae and a wide variety of substrates [3,4]. For example, geckos can run vertically at over 1 $\mathrm{m\,s^{-1}}$ and can carry over twice their body weight up smooth, vertical surfaces [5,6].

Critical to the utility of this adhesive system to the gecko is that adhesion is controllably reversible. For locomotion, an animal must be able to both stick and unstick its feet quickly. Towards this end, the adhesion of gecko setae is highly anisotropic. Setae are non-adhesive in their default state [7]. Autumn *et al.* [4] found that sticking requires a loading force perpendicular to the contact surface ('normal preload') and a short drag parallel to the contact surface ('lateral pull'). These actions mechanically prime the seta to stick, presumably by increasing the contact area of each spatula with the substrate or by increasing the number of spatulae in contact with the substrate. Spatulae are naturally curved such that their edges first contact a substrate, and the mechanical priming enables the paddle areas of the spatulae to make contact and thereby increase the adhesive force. The seta must be properly oriented towards the substrate for the mechanical prime to work. The spatular tuft at the end of the seta should be grossly oriented towards the surface for proper adhesion [4].

The pitch angle between a seta's stalk and the substrate also affects adhesion (see figure 1 for a diagram of pitch angle). Tests investigating the pitch angle at detachment found a dramatic cut-off angle, above which the seta detaches with minimal pull-off force [4]. During each step, the gecko's toes curl away from the substrate and peel off the adhesive pads on each toe. The quick, angle-dependent release mechanism enables detachment with little pull-off force. If large pull-off forces were required to remove the adhesive from a substrate, it would destabilize the animal [8], and such destabilizing forces are not observed [6].

In this work, we conduct a detailed examination on the effect of the roll and pitch orientation angles on setae adhesion. The roll angle determines what portion of the spatular tuft, if any, is oriented towards a substrate during interaction. The pitch angle between the stalk and the substrate is known to control the release of setae, but more detailed studies varying

*Author for correspondence (ginelhill@gmail.com).
†Present address: SiTime Corporation, 990 Almanor Avenue, Sunnyvale, CA 94085, USA.

Received 14 December 2010
Accepted 14 January 2011

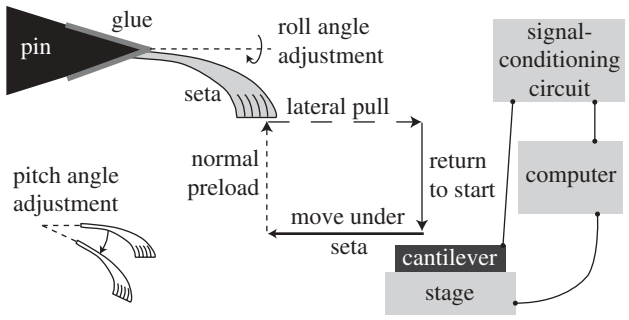

Figure 1. Experimental set-up for lateral-pull adhesive force measurements. A single seta was attached to a sharpened pin with glue. The pin was mounted on a goniometer and rotation stage (both not shown), and these were used to adjust the pitch and roll angles, respectively, of the seta relative to the cantilever. The force-sensing cantilever was mounted on a computer-controlled piezoelectric stage and moved in a box path to interact with the seta. First, the stage moved laterally under the seta and then vertically up into contact to apply normal preload force to the seta. The stage pulled laterally away from the seta in the third leg before returning to its starting position. Both lateral and normal interaction forces between the seta and the cantilever were recorded by computer using a signal-conditioning circuit to read out the cantilever's piezoresistive sensors.

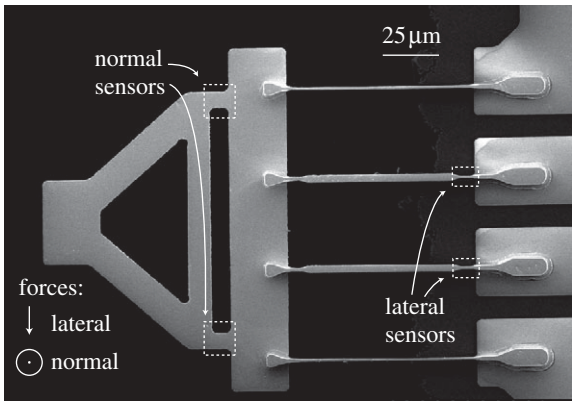

Figure 2. Image of dual-axis force-sensing cantilever by scanning electron microsopy. The broad, flat tab on the far left serves as a substrate for setae adhesion. The left half of the sensor is thin (approx. 1 µm in height) and bends out of the page in response to forces applied normal to the tab surface. The long, skinny ribs on the right are taller (10 µm) and resist normal forces but comply with lateral forces. In this way, the sensor's compliance to lateral and normal forces occurs in physically distinct regions. Piezoresistors embedded in those critical regions then separately detect applied normal and lateral forces.

pitch angle have not been performed. A thorough understanding of the role of orientation angle on the adhesion of natural setae will help facilitate the manufacture of gecko-inspired synthetic adhesives with anisotropic properties. Such an adhesive might allow robots or even humans to more easily climb walls or move along the ceiling, aid in medical devices or wound healing, or improve more mundane products such as the moveable sticky note and adhesives for wall hangings [9–11]. Additionally, the experimental data in this paper will provide additional information to constrain and improve theoretical models of gecko setae.

Ideally, investigations of the adhesive properties of geckos should simultaneously measure both the 'normal' adhesive force perpendicular to a substrate and the 'lateral' adhesive force parallel to a substrate. Gecko setae are typically loaded shear to a surface, and setal adhesive forces are stronger in the direction parallel to a substrate rather than normal to it [12]. However, both force components are important for locomotion. For example, normal forces are used to stabilize the animal in a vertical orientation during vertical motion [6]. Also, the ability to measure both force components during adhesion testing allows for better control of experimental parameters. Other laboratories have reported measurements of both components of adhesive force for macroscopic gecko samples [6,13,14], but some studies of single-seta or single-spatula adhesion report only one force component [15]. To capture the relevant information for our investigation, we employed dual-axis microscale force sensors consisting of silicon microelectromechanical system (MEMS) cantilevers with embedded piezoresistors that separately detect two components of force applied at the tip. Similar sensors were originally created for a different purpose [16,17] and were later modified and used for gecko seta measurements previously reported by our laboratory [3,4]. However, the current sensors have been subjected to more thorough calibration efforts, which should improve the accuracy of the reported adhesion forces in this work [18].

2. EXPERIMENTAL METHOD

The interaction forces generated between the seta and the substrate were measured in 'lateral-pull' experiments, as shown in figure 1. Setae were harvested from a *Gekko gecko* animal within 24–48 h of mounting. A small lamellar sample was obtained from the animal's toe pads using tweezers. From this sample, a single seta was isolated from the other setae under a dissecting microscope using sharpened pins as dissecting tools. A fine steel pin (Stahlstecknadeln Superfein, Iris, Switzerland) was sharpened using a grinding tool. The pin's tip was dipped in premixed, partially cured 5 min Epoxy (Devcon, Danvers, MA) or Gapper gap-filling adhesive (Partsmaster, Dallas, TX). The base of the seta was attached to the pin tip with the setal stalk parallel to the long axis of the pin. The glue was allowed to cure prior to experimentation. The pitch and roll angles of the seta relative to the cantilever's interaction surface were adjusted using a goniometer and rotation stage, to which the pin was affixed.

The sensors used were silicon cantilevers with embedded piezoresistive elements that separately detected forces applied perpendicular to and parallel to the surface at the cantilever tip. Figure 2 shows an image of the sensor. The unique geometry of the cantilever concentrates its mechanical compliance into physically distinct regions. The flat (1 µm in height), triangle-shaped front half of the sensor bends in response to normal forces applied at the tip, but resists bending in response to forces applied laterally. Four

long (80–200 μm), skinny (0.5–1.5 μm) and tall (10 μm) ribs connect the front half of the cantilever to the base. These ribs are stiff to normal forces but bend in response to lateral forces applied at the tip. Piezoresistive sensors are located in regions of the cantilever that experienced high stress in response to a specific force component. Thus, the embedded piezoresistors transduce forces applied at the tip of the cantilever.

The cantilever was mounted on a computer-controlled piezoelectric stage and moved in a box path to interact with the seta. A Wheatstone bridge signal-conditioning circuit converted the piezoresistance changes to voltage output, which was also recorded by computer. Lateral-pull experiments began with the cantilever moving from its starting position to directly under the seta, and then up into contact with the seta. After making contact, the cantilever continued moving upwards, thereby applying a 'normal preload' to the seta. The magnitude of this preload depended upon the relative starting positions of the cantilever and seta and the computer-programmed length of the vertical sides of the box path. Next, the cantilever moved laterally away from the seta. During lateral pulls with strong adhesion between the seta and the cantilever, the ribs would bend noticeably and the cantilever would deflect. The cantilever would reach a peak deflection and, as the stage continued to move away, slipping would occur between the seta and the cantilever tip. Eventually, the seta would fall off the edge of the cantilever tip and the stage would continue unperturbed with the lateral motion. Finally, the cantilever would return to its starting position and complete the box path.

The sensors were carefully calibrated to determine both their displacement sensitivities and stiffnesses for normal and lateral force sensing. Displacement sensitivity was determined by applying a known displacement to the cantilever tip and measuring the resulting change in voltage output from the signal-conditioning circuit. Stiffnesses were determined using two methods described by Hill [18]. First, resonant frequency measurements were used to correct for the expected variation of critical dimensions in the device geometry. Detailed finite-element models made with the improved dimensions were then used to predict the stiffnesses of each cantilever. Second, cantilever stiffnesses were measured directly with reference cantilevers to confirm the first approach.

Time traces of the force readings during an example lateral-pull experiment are shown in figure 3. For the first 5 s, the force readings are flat prior to contact. The stage begins to move vertically at 2 s on the x-axis, and continues this vertical motion until 7 s. At 5 s on the scale, the cantilever contacts the seta and experiences interaction forces, as the seta pushes back on the cantilever. The seta is curved at its branched end and thus pushes on the cantilever both vertically and horizontally, even though the stage motion is exclusively vertical at this point. At 7 s, the stage ceases vertical motion and begins pulling laterally away from the seta. The slope of both the lateral and normal force readings changes sign at this point. The seta grips the cantilever and pulls on it rather than pushing.

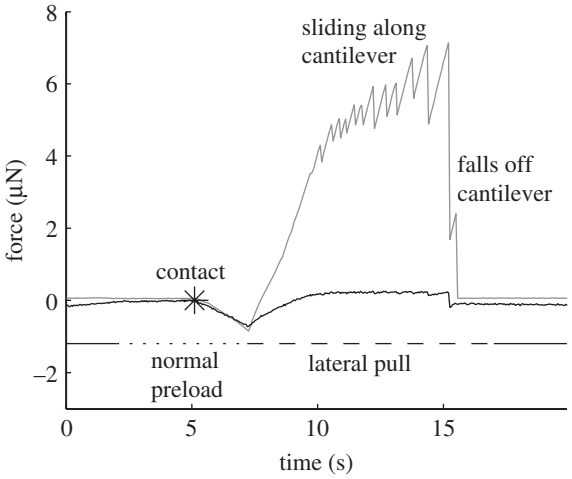

Figure 3. Lateral (grey line) and normal force (black line) readings during a lateral-pull measurement of seta adhesion. At the beginning of the experiment, the force sensors read near zero until the seta contacts the cantilever at approximately $t = 5$ s (asterisk). Normal preload continues until $t = 7$ s, which is when the lateral pull begins. Because the seta is curved at its distal end, it pushes the cantilever in both the lateral and normal directions during the normal preload stage though the stage motion was purely in the normal direction. During lateral pull, the normal and lateral interaction forces switch in sign as the seta pulls on the cantilever rather than pushes. The lateral force linearly increases with stage movement until slip–stick behaviour begins. The stick–slip behaviour continues until the seta falls off the edge of the cantilever.

Between 7 and 10 s, the lateral force rises linearly and there is no slipping observed between the cantilever and the seta. The normal force reading also changes sign during the lateral pull, settling just above zero as the seta is stretched out into a more horizontal and less curved shape and is pulling rather than pushing on the cantilever. Beginning at 10 s, the seta exhibits stick–slip motion until falling off the edge at approximately 15 s. The cantilever might actually oscillate during the slip–stick events, but the data acquisition sampling rate was too slow to follow resonant oscillation of the cantilever. Most data were taken at 1 kHz, though some were taken at slower rates between 20 and 50 Hz, and the sensors have resonant frequencies well above 5 kHz. After the seta drops off the cantilever in the lateral-pull experiment, both force readings return to baseline values and the cantilever returns to its starting position.

For a given lateral-pull measurement, the peak value of the lateral force sensor was recorded to determine the maximum observed lateral force generated during the measurement. Also, the most negative value for the normal sensor was used to indicate the normal preload force applied and the normal force readings were fitted to determine the contact point between the seta and the cantilever. Adjustments were made to compensate for background readings from both sensors using data taken when the cantilever was far from the seta in the box path. These background readings were non-zero primarily because of drift in the piezoresistive sensors. In each signal-conditioning

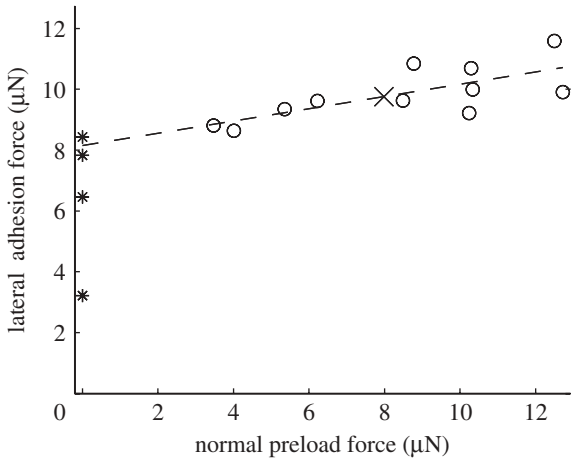

Figure 4. Lateral adhesion force versus normal preload for a single seta. Each datum point represents a separate box path measurement. The maximum lateral adhesive force measured during a run is shown on the *y*-axis versus the magnitude of the normal preload force achieved just prior to the lateral pull. At preload values near zero, the lateral force measured was highly variable. Excluding these low-preload runs, a line was fitted to the remaining data and evaluated at the desired preload value (in this case, $F_{\text{preload}} = 8\ \mu\text{N}$) to extract the lateral adhesive force at a specific preload from these multiple measurements at various moderate preloads. Open circles, data used for fit; asterisks, data excluded from fit; dashed line, fit; cross, extracted lateral force.

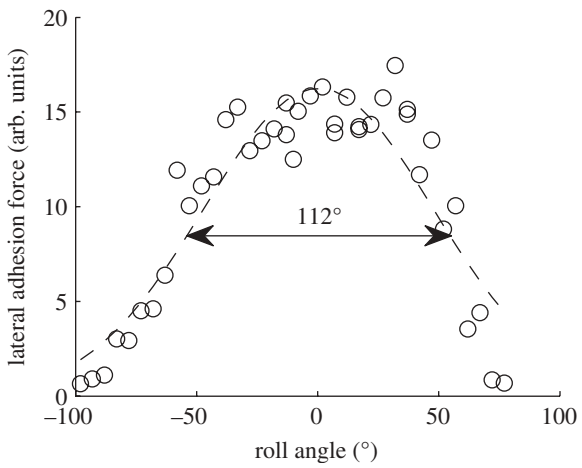

Figure 5. Lateral adhesion versus roll angle for a single seta. Both data points (circles) as well as Gaussian fit (dashed line) are shown. The FWHM range of the fit is 112°.

circuit, the piezoresistor was balanced by adjusting the corresponding potentiometer prior to beginning a series of measurements. However, measurements were often conducted sequentially without rebalancing the Wheatstone bridge. Thus, the baseline force reading was often slightly offset from zero. For each lateral-pull measurement, all the force readings were adjusted to correct for the average baseline value as determined by sample values from the beginning and the end of the run.

3. NORMAL PRELOAD EXPERIMENTS

We investigated the effect of normal preload on lateral adhesive force measurements by methodically varying the normal preload applied in lateral-pull experiments. Figure 4 shows data from an example measurement with normal preload force on the *x*-axis and the measured lateral adhesive force on the *y*-axis. Normal preload increases the observed lateral adhesion above the adhesion measured with no preload, which is the *y*-intercept value on the graph. For this orientation of seta and cantilever, the amount of normal preload has a modest influence on the lateral force measured. For other orientations with less lateral adhesion force, the normal preload had a larger influence relative to the lateral force measured with no preload.

In later experiments, the normal preload was standardized for a particular orientation angle of the seta. The lateral force measurements recorded at exactly zero normal preload varied widely as it was difficult to apply no preload and yet still have contact between the seta and the substrate. When aiming for zero preload force, in some instances, the seta would just contact the substrate and ultimately stick, while in other runs it would miss entirely. To minimize the ambiguity of these experiments with low preload, data points taken near zero preload were excluded and a line was fitted to the data points with higher normal preload. The lateral adhesive force on the fit line at the specified normal preload was then attributed to the particular orientation of the seta. In this example, the specified preload was approximately 8 μN (or 10 μm displacement for this cantilever tip) and the lateral force attributed to this orientation was approximately 8.5 μN.

Previous work investigated the effect of normal preload on the *normal* force required to detach a seta [19] and found that the normal force required for detachment of a seta increased with the normal preload applied up to a point. Liang [19] found that a maximal normal detachment force could also be achieved with a short lateral pull instead of normal preload. In other words, high levels of normal adhesive force could be achieved either by using moderate normal preload forces or by performing a short lateral drag of the seta. In contrast, the measurements in this work show that normal preload does have an effect on the *lateral* adhesion force measured and that this effect is not removed or replicated by lateral motion or pulling. While it is possible that the effect of normal preload on lateral adhesion would level off at higher preloads, these sensors were too fragile and compliant for safe investigation of larger preload forces. Stiffer cantilevers might be used in future experiments to investigate the influence of larger normal preload forces on lateral adhesive force of gecko setae.

4. EFFECTS OF ROLL ANGLE

The effect of the roll orientation angle on the lateral adhesive force of a gecko seta was examined. To change the roll angle of the seta (figure 1), the pin on which the seta was mounted was rotated about its long axis using a rotation stage. The results of an initial study of roll angle are shown in figure 5. Lateral adhesive force is on the *y*-axis while roll angle is on

the x-axis. The y-axis of this graph is in arbitrary units, as the cantilever used was broken prior to calibration. However, only one cantilever was used for acquiring data for this seta, so the values may be safely compared with one another and the shape of the graph remains accurate. Normal preload was approximately held constant but not methodically varied for each orientation angle in this dataset. The distribution of data points is roughly a Gaussian shape with a slightly flattened top. When fitted with a Gaussian, the full-width, half-maximum (FWHM) angle range is 112°. Near-maximum adhesion is found over a narrower subjective range between −43° and +43°. Between roll angles −85° and +85°, lateral adhesion is enhanced from the baseline value observed when the spatular tuft at the end of the seta is grossly misoriented away from the substrate.

Visual observations of the seta–substrate interactions during experiments revealed why imperfectly aligned setae exhibited near-maximum adhesion values. For a seta at an initial roll angle of 30° from optimum, a minority of its outer spatulae would initially make contact with the substrate. During the lateral pull, these would catch hold, and torque the seta such that it would rotate the tuft into ideal position. With most spatulae then properly oriented for contact with the substrate, the observed adhesion was near maximum. For initial roll angles farther from optimum, the few spatulae initially in contact did not provide enough torque to fully rotate the tuft into ideal position. However, if these available setae caught hold, lateral adhesion was still enhanced above frictional values. Outside of the −85° and +85° roll angle range of enhanced adhesion for this seta, either no spatula made contact with the substrate or those that did never oriented with their flat portion parallel to the substrate and caught hold. Alternatively, the spatular tuft of this seta can be thought of as splaying out over a 170° range, with optimum adhesion possible over the central 85°.

Subsequent measurements of the same seta in the weeks following initial measurement showed curves with similar shape. While the maximum force on a given day was roughly consistent across the ideal angle range, there was substantial variation on different days in the average maximum value for the same seta stored in a standard laboratory environment. The FWHM angle range varied from 97° to 105°, reduced from the first measurement. Humidity has been reported to affect the force required to pull a seta off a substrate [20] and might also affect the rotational stiffness and other mechanical properties of the keratin seta.

A more detailed study of the effect of roll angle on lateral adhesion was undertaken on a second seta using a well-calibrated sensor and multiple measurements at various normal preloads. Figure 6 shows the combined effects of roll angle and normal preload for this seta. This seta has a narrower tolerance to roll angle variations than the prior seta, with a FWHM range of 67°. As discussed earlier, higher levels of normal preload modestly increase the observed lateral adhesive force. This enhancement can be more significant as a percentage change from the low-preload value when the seta is poorly oriented and overall adhesion forces are low. However, the effect of roll angle on lateral adhesive force appears qualitatively similar for different values of the normal preload.

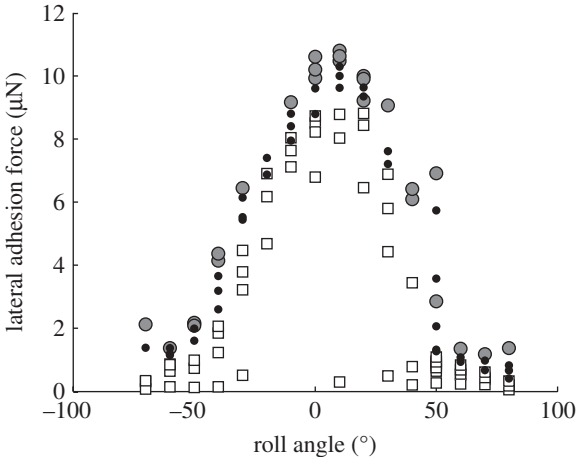

Figure 6. Effects of normal preload and roll angle on lateral adhesion force of a single seta. For each roll angle, multiple measurements were taken with different values of normal preload revealing that normal preload causes a modest increase in the observed lateral adhesion. However, the shape of the response is consistent at different preloads, excepting some irregular behaviour at low preload levels when insufficient contact was made for adhesion. This seta has a narrower roll angle tolerance than the seta measured in figure 5, with the FWHM range of 67° found using a Gaussian fit to the extracted data with 8 μN normal preload. Grey circles, 10 + μN; black circles, 5–10 μN; open squares, 0–5 μN.

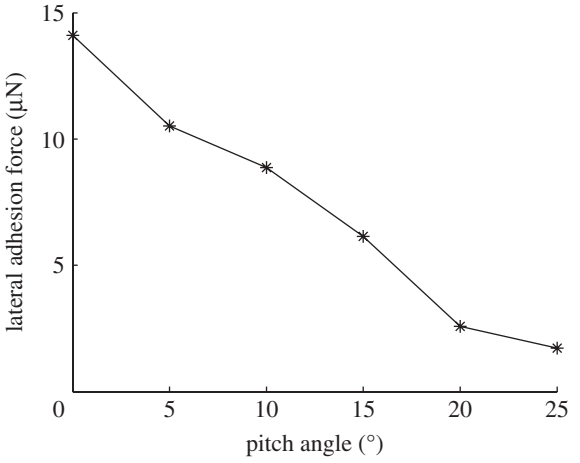

Figure 7. Lateral adhesion versus pitch angle for a single seta. Adhesion decreases smoothly from its maximum value at 0° pitch to near-baseline levels at 25° pitch.

5. EFFECTS OF PITCH ANGLE

The effect of the pitch orientation angle on lateral adhesive force was investigated. The pitch angle between the stalk of a seta (figure 1) and the substrate was changed by adjusting using the goniometer on which the seta, mount pin and rotation stage were all mounted. Figure 7 shows the lateral adhesive force versus pitch angle for a single seta. Values shown

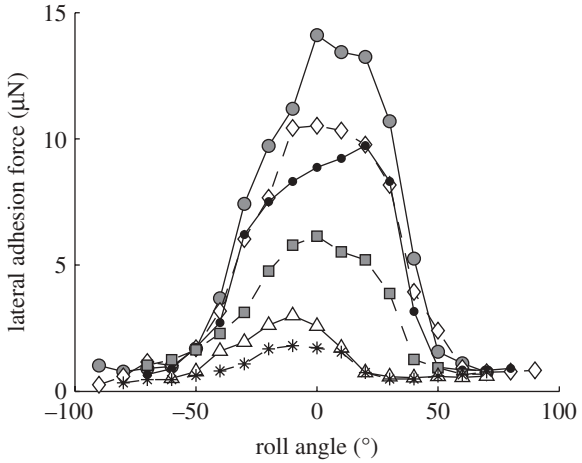

Figure 8. Pitch and roll angle effects on lateral adhesion force from a single seta. Lateral adhesion force is shown as a function of roll angle for a variety of pitches. Maximum adhesion is observed for the lowest pitch angle of 0°, and adhesion decreases with increasing pitch until minimal adhesion above the baseline level is observed at 25° pitch. The shape of the roll angle dependence stays relatively consistent at various pitches as the peak adhesion decreases. Grey circles, 0°; diamonds, 5°; black circles, 10°; filled squares, 15°; triangles, 20°; asterisks, 25°.

correspond to a constant normal preload and were extracted from multiple measurements taken at each orientation with various preloads. The maximum lateral adhesion of 14 μN occurs at a pitch angle of 0°, meaning that the stalk of the seta is parallel to the substrate. With increasing pitch angle, the lateral adhesive force drops smoothly. At 25°, the adhesion was reduced to near the background frictional values.

The interplay between pitch and roll angle effects on lateral adhesion force is displayed in figure 8. As pitch increases, the lateral adhesive force decreases at all roll angles. The shape of the roll angle dependence is mostly preserved at different pitches, though the roll angle for peak adhesion shifts somewhat with increasing pitch.

These results on the effect of pitch angle on lateral adhesion are consistent with prior work on pitch angle but provide more detail and use a slightly different experimental method. Previous researchers on both single setae and whole geckos adjusted the pitch angle after attachment and found that, at a critical angle, the gecko adhesive detaches. This critical release angle was found to vary by species [21]. Single seta experiments made with a wire gauge report a consistent detachment angle of 30° for *Gekko gecko* setae independent of normal force. Experiments measuring whole *Gekko gecko* animals suspended by the attachment of a rear toe to a glass slide mounted on a rotation stage found that the animal would fall when the slide was adjusted to an angle of 25° from vertical [22]. In contrast to those experiments that adjust the pitch angle after attachment, the experiments in this paper present the seta to the surface at a specific angle and measure the resulting interaction force. As well, they provide more detail about the effect of pitch on lateral adhesion of setae by showing the decline in adhesive force with increasing pitch, rather than just revealing an angle of detachment. Also, these experiments show that, for maximum adhesion, the seta should be as close to parallel with the surface as possible.

6. CONCLUSION

In this work, we described the interplay of pitch and roll orientation angle on single gecko setae adhesion using a well-calibrated dual-axis microscale force sensor. We found that the maximum lateral adhesion observed is highly sensitive to pitch angle, with a maximum setae adhesion found with the seta's stalk parallel to the substrate. There is a smooth fall-off of adhesion strength as a function of pitch angle until the seta nears its detachment angle. In contrast, setae adhesion is tolerant of moderate roll angle misalignment, with a FWHM over 60°. The effects of normal preload on the lateral adhesive force were also investigated. Normal preload has a modest but consistent enhancement effect on the observed lateral adhesive force provided that sufficient physical contact was made between the seta and the substrate. Roll orientation angle dependence is substantially maintained at varying normal preloads. As expected, the interaction between pitch and roll shows dramatic changes in lateral adhesion force. To achieve optimal adhesion of an individual seta, careful control of the seta pitch and only rough control of the seta roll angle are necessary.

Together, these data show that the attachment of gecko setae is robust with respect to roll angle but highly sensitive to pitch angle. Rather than by pulling, gecko setae are released by an angle adjustment. Recent theoretical work has explored the strong pitch angle dependence of gecko adhesion and postulates that pretension of the spatulae plays a critical role [23]. Pitch angle dependence in particular is extremely important for providing a detachment mechanism with minimal pull-off force. This characteristic is critical to locomotion but might also be useful in other applications to prevent substrate damage or allow easy removal of adhesives, particularly against forces acting predominantly in one direction, such as gravity.

The robustness of adhesion at various roll angles may be beneficial in adhering to rough surfaces [24,25], and may also improve adhesion tolerance to moderate misalignment. This tolerance is particularly useful to the gecko given that both its feet and the majority of substrates in its natural environment are not planar. There has been considerable work modelling the adhesive properties of gecko setae [14,23,26–30]. However, thus far, the tolerance to roll angle variations in gecko adhesion seems to be a useful feature that has not been fully addressed in theoretical models of the setae. We note in this work that the range of roll angle tolerance in adhesion roughly correlates with the spread angle of the spatular tuft at the end of each seta. However, visual observations of setae during lateral-pull experiments also revealed that some roll angle tolerance is achieved by rotation to a more optimal angle during the attachment process. The data in this paper provide additional information and detail on the adhesive properties of natural setae to aid in the creation of more accurate and representative theoretical models of gecko setae.

The maximum adhesive force observed in these studies is 14 μN. This result is significantly less than the adhesive force reported by previous research using earlier versions of the dual-axis MEMS force sensor [4]. Autumn *et al.* [4] reported a lateral adhesion force of over 100 μN for a single *Gekko gecko* seta, and they calibrated the stiffness of their sensor using a commercial force calibration cantilever as a reference spring. However, the calibration of microscale cantilevers is a notorious problem, and recent work has found that the nominal values of commercial cantilevers may be off by over 100 per cent [31]. It is also possible that there is significant natural variation in setae and that both measurements are accurate. However, the force-sensing cantilevers used in the present work were subject to a more extensive calibration methodology involving both resonant frequency-corrected finite-element modelling and the use of reference cantilevers [18]. The adhesion forces presented in this work are more consistent with the adhesive forces measured subsequently by a different method in Peattie [21], which found an average lateral adhesive force of 20 ± 16 μN for *Gekko gecko* setae. They are also consistent with a recent theoretical model of the gecko adhesive [28].

A wealth of recent research has been devoted to synthetically mimicking the gecko adhesive [32–43]. However, many early synthetics did not display or address anisotropic adhesion and angle-dependent release mechanisms, which are critical for controllable attachment and release during locomotion. More recent work on synthetic gecko-inspired adhesives and their mechanics has begun to investigate and demonstrate anisotropic properties [44–51], though no synthetic has yet captured the full attributes of the original. The results presented here on the effect of orientation angle on single hair adhesion for natural setae may inform further work on synthetic adhesives inspired by the gecko. Especially for synthetic adhesives designed for climbing robots, or for reusable adhesives, controllable attachment and release are paramount. If excessive force is required to remove an adhesive, a climber would be thrown off balance, a moveable note might be destroyed or a wound might be reopened. Harnessing the release mechanism exploited by geckos would be a tremendous advancement for synthetic dry adhesives.

This material is based upon work supported by the National Science Foundation under the Center for Integrated Nanosystems (COINS, grant no. ECS-0425914) and the National Interdisciplinary Research Team (NIRT, grant no. 0708367). Work was performed, in part, at the Stanford Nanofabrication Facility (a member of the National Nanotechnology Infrastructure Network), which is supported by the National Science Foundation under grant ECS-9731293, its laboratory members, and the industrial members of the Stanford Center for Integrated Systems. The Kirby Stanford Graduate Fellowship and a Stanford DARE Fellowship partially supported G.H. and D.S., respectively.

REFERENCES

1 Ruibal, R. & Ernst, V. 1965 Structure of digital setae of lizards. *J. Morphol.* **117**, 271–294. (doi:10.1002/jmor.1051170302)

2 Maderson, P. F. 1964 Keratinized epidermal derivatives as aid to climbing in gekkonid lizards. *Nature* **203**, 780–781. (doi:10.1038/203780a0)

3 Autumn, K. *et al.* 2002 Evidence for van der Waals adhesion in gecko setae. *Proc. Natl Acad. Sci. USA* **99**, 12 252–12 256. (doi:10.1073/pnas.192252799)

4 Autumn, K., Liang, Y. A., Hsieh, S. T., Zesch, W., Chan, W. P., Kenny, T. W., Fearing, R. & Full, R. J. 2000 Adhesive force of a single gecko foot-hair. *Nature* **405**, 681–685. (doi:10.1038/35015073)

5 Irschick, D. J., Vanhooydonck, B., Hertel, A. & Andronescu, A. 2003 Effects of loading and size on maximum power output and gait characteristics in geckos. *J. Exp. Biol.* **206**, 3923–3934. (doi:10.1242/jeb.00617)

6 Autumn, K., Hsieh, S. T., Dudek, D. M., Chen, J., Chitaphan, C. & Full, R. J. 2006 Dynamics of geckos running vertically. *J. Exp. Biol.* **209**, 260–272. (doi:10.1242/jeb.01980)

7 Autumn, K. & Hansen, W. 2006 Ultrahydrophobicity indicates a non-adhesive default state in gecko setae. *J. Comp. Physiol. A* **192**, 1205–1212. (doi:10.1007/s00359-006-0149-y)

8 Kim, S., Spenko, M., Trujillo, S., Heyneman, B., Santos, D. & Cutkosky, M. R. 2008 Smooth vertical surface climbing with directional adhesion. *IEEE Trans. Rob.* **24**, 65–75. (doi:10.1109/TRO.2007.909786)

9 del Campo, A. & Arzt, E. 2007 Design parameters and current fabrication approaches for developing bioinspired dry adhesives. *Macromol. Biosci.* **7**, 118–127. (doi:10.1002/mabi.200600214)

10 Santos, D., Spenko, M., Parness, A., Kim, S. & Cutkosky, M. 2007 Directional adhesion for climbing: theoretical and practical considerations. *J. Adhes. Sci. Technol.* **21**, 1317–1341. (doi:10.1163/156856107782328399)

11 Mahdavi, A. *et al.* 2008 A biodegradable and biocompatible gecko-inspired tissue adhesive. *Proc. Natl Acad. Sci. USA* **105**, 2307–2312. (doi:10.1073/pnas.0712117105)

12 Tian, Y., Pesika, N., Zeng, H., Rosenberg, K., Zhao, B., McGuiggan, P., Autumn, K. & Israelachvili, J. 2006 Adhesion and friction in a gecko toe attachment and detachment. *Proc. Natl Acad. Sci. USA* **103**, 19 320–19 325. (doi:10.1073/pnas.0608841103)

13 Sponberg, S., Hansen, W., Peattie, A. & Autumn, K. 2001 Dynamics of isolated gecko setal arrays. *Am. Zool.* **41**, 1594.

14 Zhao, B. X., Pesika, N., Rosenberg, K., Tian, Y., Zeng, H. B., McGuiggan, P., Autumn, K. & Israelachvili, J. 2008 Adhesion and friction force coupling of gecko setal arrays: implications for structured adhesive surfaces. *Langmuir* **24**, 1517–1524. (doi:10.1021/la702126k)

15 Huber, G., Gorb, S. N., Spolenak, R. & Arzt, E. 2005 Resolving the nanoscale adhesion of individual gecko spatulae by atomic force microscopy. *Biol. Lett.* **1**, 2–4. (doi:10.1098/rsbl.2004.0254)

16 Chui, B. W., Kenny, T. W., Mamin, H. J., Terris, B. D. & Rugar, D. 1998 Independent detection of vertical and lateral forces with a sidewall-implanted dual-axis piezoresistive cantilever. *Appl. Phys. Lett.* **72**, 1388–1390. (doi:10.1063/1.121064)

17 Chui, B. W., Mamin, H. J., Tetris, B. D., Rugar, D. & Kenny, T. W. 1998 Sidewall-implanted dual-axis piezoresistive cantilever for AFM data storage readback and tracking. In *Proc. 11th Annual IEEE Micro Electro Mechanical Systems (MEMS) Workshop, Heidelberg, Germany, 25–29 January 1998*, pp. 12–17.

18 Hill, G. C. 2009 Dual-axis MEMS force sensors for gecko adhesion studies. PhD thesis, Stanford University, Stanford, CA.

19 Liang, Y. 2001 Piezoresistive cantilevers for force measurements. PhD thesis, Stanford University, Stanford, CA.

20 Huber, G., Mantz, H., Spolenak, R., Mecke, K., Jacobs, K., Gorb, S. N. & Arzt, E. 2005 Evidence for capillarity contributions to gecko adhesion from single spatula nanomechanical measurements. *Proc. Natl Acad. Sci. USA* **102**, 16 293–16 296. (doi:10.1073/pnas.0506328102)

21 Peattie, A. 2007 The function and evolution of gekkotan adhesive feet. PhD thesis, University of California, Berkeley, CA.

22 Autumn, K., Dittmore, A., Santos, D., Spenko, M. & Cutkosky, M. 2006 Frictional adhesion: a new angle on gecko attachment. *J. Exp. Biol.* **209**, 3569–3579. (doi:10.1242/jeb.02486)

23 Chen, B., Wu, P. D. & Gao, H. J. 2009 Pre-tension generates strongly reversible adhesion of a spatula pad on substrate. *J. R. Soc. Interface* **6**, 529–537. (doi:10.1098/rsif.2008.0322)

24 Russell, A. P., Johnson, M. K. & Delannoy, S. M. 2007 Insights from studies of gecko-inspired adhesion and their impact on our understanding of the evolution of the gekkotan adhesive system. *J. Adhes. Sci. Technol.* **21**, 1119–1143. (doi:10.1163/156856107782328371)

25 Vanhooydonck, B., Andronescu, A., Herrel, A. & Irschick, D. J. 2005 Effects of substrate structure on speed and acceleration capacity in climbing geckos. *Biol. J. Linn. Soc.* **85**, 385–393. (doi:10.1111/j.1095-8312.2005.00495.x)

26 Yao, H. & Gao, H. 2006 Mechanics of robust and releasable adhesion in biology: bottom-up designed hierarchical structures of gecko. *J. Mech. Phys. Solids* **54**, 1120–1146. (doi:10.1016/j.jmps.2006.01.002)

27 Kim, T. W. & Bhushan, B. 2007 Adhesion analysis of multi-level hierarchical attachment system contacting with a rough surface. *J. Adhes. Sci. Technol.* **21**, 1–20. (doi:10.1163/156856107779976097)

28 Chen, B., Wu, P. D. & Gao, H. 2008 Hierarchical modelling of attachment and detachment mechanisms of gecko toe adhesion. *Proc. R. Soc. A* **462**, 1639–1652. (doi:10.1098/rspa.2007.0350)

29 Zhao, B. X., Pesika, N., Zeng, H. B., Wei, Z. S., Chen, Y. F., Autumn, K., Turner, K. & Israelachvili, J. 2009 Role of tilted adhesion fibrils (setae) in the adhesion and locomotion of gecko-like systems. *J. Phys. Chem. B* **113**, 3615–3621. (doi:10.1021/jp806079d)

30 Yao, H., Chen, S., Guduru, P. R. & Gao, H. 2009 Orientation-dependent adhesion strength of a rigid cylinder in non-slipping contact with a transversely isotropic half-space. *Int. J. Solids Struct.* **46**, 1167–1175. (doi:10.1016/j.ijsolstr.2008.10.011)

31 Langlois, D., Shaw, G. A., Kramer, J. A., Pratt, J. R. & Hurley, D. C. 2007 Spring constant calibration of atomic force microscopy cantilevers with a piezoresistive transfer standard. *Rev. Sci. Instrum.* **78**, 093 705–093 710. (doi:10.1063/1.2785413)

32 Yurdumakan, B., Raravikar, N. R., Ajayan, P. M. & Dhinojwala, A. 2005 Synthetic gecko foot-hairs from multiwalled carbon nanotubes. *Chem. Commun.* **30**, 3799–3801. (doi:10.1039/b506047h)

33 Majidi, C. S., Groff, R. E. & Fearing, R. S. 2005 Attachment of fiber array adhesive through side contact. *J. Appl. Phys.* **98**, 103521. (doi:10.1063/1.2128697)

34 Northen, M. T. & Turner, K. L. 2005 A batch fabricated biomimetic dry adhesive. *Nanotechnology* **16**, 1159–1166. (doi:10.1088/0957-4484/16/8/030)

35 Sitti, M. & Fearing, R. S. 2003 Synthetic gecko foot-hair micro/nano-structures as dry adhesives. *J. Adhes. Sci. Technol.* **17**, 1055–1073. (doi:10.1163/156856103322113788)

36 del Campo, A., Greiner, C., Alvarez, I. & Arzt, E. 2007 Patterned surfaces with pillars with controlled 3D geometry mimicking bioattachment devices. *Adv. Mater.* **19**, 1973. (doi:10.1002/adma.200602476)

37 Ge, L., Sethi, S., Ci, L., Ajayan, P. M. & Dhinojwala, A. 2007 Carbon nanotube-based synthetic gecko tapes. *Proc. Natl Acad. Sci. USA* **104**, 10 792–10 795. (doi:10.1073/pnas.0703505104)

38 Glassmaker, N. J., Jagota, A., Hui, C. Y., Noderer, W. L. & Chaudhury, M. K. 2007 Biologically inspired crack trapping for enhanced adhesion. *Proc. Natl Acad. Sci. USA* **104**, 10 786–10 791. (doi:10.1073/pnas.0703762104)

39 Kim, S., Aksakm, B. & Sitti, M. 2007 Enhanced friction of elastomer microfiber adhesives with spatulate tips. *Appl. Phys. Lett.* **91**, 221913. (doi:10.1063/1.2820755)

40 Lee, H., Lee, B. P. & Messersmith, P. B. 2007 A reversible wet/dry adhesive inspired by mussels and geckos. *Nature* **448**, 338–341. (doi:10.1038/nature05968)

41 Cho, W. K. & Choi, I. S. 2008 Fabrication of hairy polymeric films inspired by geckos: wetting and high adhesion properties. *Adv. Funct. Mater.* **18**, 1089–1096. (doi:10.1002/adfm.200701454)

42 Kim, S., Kustandi, T. S. & Yi, D. K. 2008 Synthesis of artificial polymeric nanopillars for clean and reusable adhesives. *J. Nanosci. Nanotechnol.* **8**, 4779–4782. (doi:10.1166/jnn.2008.IC45)

43 Northen, M. T., Greiner, C., Arzt, E. & Turner, K. L. 2008 A Gecko-inspired reversible adhesive. *Adv. Mater.* **20**, 3905. (doi:10.1002/adma.200801340)

44 Chen, S. H. & Gao, H. J. 2007 Bio-inspired mechanics of reversible adhesion: orientation-dependent adhesion strength for non-slipping adhesive contact with transversely isotropic elastic materials. *J. Mech. Phys. Solids* **55**, 1001–1015. (doi:10.1016/j.jmps.2006.10.008)

45 Jeong, H. E., Lee, J. K., Kim, H. N., Moon, S. H. & Suh, K. Y. 2009 A nontransferring dry adhesive with hierarchical polymer nanohairs. *Proc. Natl Acad. Sci. USA* **106**, 5639–5644. (doi:10.1073/pnas.0900323106)

46 Qu, L. T., Dai, L. M., Stone, M., Xia, Z. H. & Wang, Z. L. 2008 Carbon nanotube arrays with strong shear binding-on and easy normal lifting-off. *Science* **322**, 238–242. (doi:10.1126/science.1159503)

47 Lee, J. H. & Fearing, R. S. 2008 Directional adhesion of gecko-inspired angled microfiber arrays. *Appl. Phys. Lett.* **93**, 191910. (doi:10.1063/1.3006334)

48 Murphy, M. P., Aksak, B. & Sitti, M. 2007 Adhesion and anisotropic friction enhancements of angled heterogeneous micro-fiber arrays with spherical and spatula tips. *J. Adhes. Sci. Technol.* **21**, 1281–1296. (doi:10.1163/156856107782328380)

49 Parness, A., Soto, D., Esparza, N., Gravish, N., Wilkinson, M., Autumn, K. & Cutkosky, M. 2009 A microfabricated wedge-shaped adhesive array displaying gecko-like dynamic adhesion, directionality and long lifetime. *J. R. Soc. Interface* **6**, 1223–1232. (doi:10.1098/rsif.2009.0048)

50 Lee, J., Majidi, C., Schubert, B. & Fearing, R. S. 2008 Sliding-induced adhesion of stiff polymer microfibre arrays. I. Macroscale behaviour. *J. R. Soc. Interface* **5**, 835–844. (doi:10.1098/rsif.2007.1308)

51 Schubert, B., Lee, J., Majidi, C. & Fearing, R. S. 2008 Sliding-induced adhesion of stiff polymer microfibre arrays. II. Microscale behaviour. *J. R. Soc. Interface* **5**, 845–853. (doi:10.1098/rsif.2007.1309)